1990-03-01

Dictyostelium discoideum plasma membranes contain an actin-nucleating activity that requires ponticulin, an integral membrane glycoprotein

A. Shariff

Et al.

Dictyostelium discoideum Plasma Membranes Contain an Actin-nucleating Activity That Requires Ponticulin, an Integral Membrane Glycoprotein

Aneesa Shariff and Elizabeth J. Luna

Worcester Foundation for Experimental Biology, Shrewsbury, Massachusetts 01545

Abstract. In previous equilibrium binding studies, *Dictyostelium discoideum* plasma membranes have been shown to bind actin and to recruit actin into filaments at the membrane surface. However, little is known about the kinetic pathway(s) through which actin assembles at these, or other, membranes. We have used actin fluorescently labeled with *N*-(1-pyrenyl)iodoacetamide to examine the kinetics of actin assembly in the presence of *D. discoideum* plasma membranes. We find that these membranes increase the rate of actin polymerization. The rate of membrane-mediated actin polymerization is linearly dependent on membrane protein concentrations up to 20 μg/ml. Nucleation (the association of activated actin monomers into oligomers) appears to be the primary step of polymerization that is accelerated. A sole effect on the initial salt-induced actin conformational change (activation) is ruled out because membranes accelerate the polymerization of pre-activated actin as well as actin activated in the presence of membranes. Elongation of preexisting filaments also is not the major step of polymerization facilitated by membranes since membranes stripped of all peripheral components, including actin, increase the rate of actin assembly to about the same extent as do membranes containing small amounts of endogenous actin. Acceleration of the nucleation step by membranes also is supported by an analysis of the dependence of polymerization lag time on actin concentration. The barbed ends of membrane-induced actin nuclei are not obstructed by the membranes because the barbed end blocking agent, cytochalasin D, reduces the rate of membrane-mediated actin nucleation. Similarly, the pointed ends of the nuclei are not blocked by membranes since the depolymerization rate of gelsolin-capped actin is unchanged in the presence of membranes. These results are consistent with previous observations of lateral interactions between membranes and actin filaments. These results also are consistent with two predictions from a model based on equilibrium binding studies; i.e., that plasma membranes should nucleate actin assembly and that membrane-bound actin nuclei should have both ends free (Schwartz, M. A., and E. J. Luna. 1988. *J. Cell Biol.* 107:201–209).

Integral membrane proteins mediate the actin nucleation activity because activity is eliminated by heat denaturation, treatment with reducing agents, or proteolysis of membranes. Activity also is abolished by solubilization with octylglucoside but is reconstituted upon removal or dilution of the detergent. Ponticulin, the major actin-binding protein in plasma membranes, appears to be necessary for nucleation activity since activity is not reconstituted from detergent extracts depleted of ponticulin.

CELLULAR responses to chemotactic and phagocytic factors include large, rapid increases in actin polymerization and in the amounts of actin associated with the cytoskeleton (for review, see references 4, 19, 47, 51, 61). Actin appears to be actively recruited to plasma membrane sites, including the anterior ends of locomoting cells, phagocytic cups, and adherens junctions (for review, see 9, 10, 27, 45, 62). Chemotactic factors, in particular, are reported to trigger the formation of new actin nucleation sites with free barbed ends; i.e., the increased actin polymerization during chemotaxis is inhibited by the barbed-end capping agent, cytochalasin D (CD)[1] (11, 32). Although the intracellular location of these actin nucleation sites is unknown, the rapidity (3–10 s) of the actin polymerization response (32, 49, 63) suggests an immediate involvement of the plasma membrane in the signaling process.

D. discoideum plasma membranes are known to bind and assemble actin filaments in vitro (44, 58, 66). The specific binding of actin to membranes is of high avidity and appears

1. *Abbreviations used in this paper*: CD, cytochalasin D; NEM, *N*-ethyl maleimide; OG, octylglucoside; pyrene, actin labeled with *N*-(1-pyrenyl)iodoacetamide-actin.

to involve the sides, rather than the ends, of the filaments (3, 30, 44, 58). Both preformed F-actin and polymerizing G-actin bind to these membranes within a few minutes at 18–22°C (58); by contrast, the off rate is undetectable under physiological conditions (44). Most of the actin-binding activity appears to be mediated by integral membrane proteins since activity resists extraction by chaotropes but is sensitive to proteolysis, heat denaturation, and reducing agents (43, 44, 58, 66). Several low molecular mass actin-binding proteins associated with *Dictyostelium* membranes have been described (7, 55, 56, 66, 74). In particular, ponticulin, a 17-kD transmembrane glycoprotein, is thought to be responsible for most of the in vitro actin-binding activity of *Dictyostelium* plasma membranes. Ponticulin is the major protein isolated by actin affinity chromatography of octylglucoside (OG)–solubilized plasma membranes, and monovalent antibody fragments directed against the cytoplasmic portion of this protein inhibit 96% of the actin-membrane binding in sedimentation assays (74). An abundant membrane protein, ponticulin constitutes 0.4–1.0% of the total protein in plasma membranes from log-phase cells (74). During development, the amount of ponticulin in the plasma membrane increases two- to threefold during the time that cells are engaged in aggregation streaming, suggesting that this protein may play a role in the enhanced cell motility and/or cell-cell adhesion characteristic of this developmental stage (35). In fact, high concentrations of ponticulin are observed in the plasma membrane at sites of lateral cell-cell contact and in arched areas reminiscent of early pseudopods (75). As ponticulin also is a component of the Triton-insoluble cytoskeleton (75), this protein is ideally situated for a role in signal transduction during cell-cell adhesion and cell translocation.

Equilibrium binding studies indicate that *Dictyostelium* plasma membranes induce actin polymerization at subcritical actin concentrations and that the actin-binding and actin-assembly activities of the membranes are tightly coupled (58, 59). To explain the tight coupling between binding and polymerization, Schwartz and Luna (59) have proposed a model for actin-membrane binding that is consistent with F-actin structure, membrane binding to the sides of actin filaments, and Hill plots of binding data that indicate that at least three actin monomers are involved in the assembly of a stable actin-membrane complex. The model proposes that adjacent actin monomers on one side of the filament bind to clustered membrane sites, giving rise to a nucleus stabilized by lateral associations with the membrane. Because the angle between successive subunits in an actin filament approaches 180° (23), the smallest nucleus that could be stabilized by such associations is an actin trimer bound to two membrane sites. Membranes are predicted to increase the rate of actin polymerization, either by potentiating the formation of actin nuclei, by stabilizing spontaneously assembled nuclei, or both. A second prediction of the model is that the putative membrane-bound actin trimers should have both ends free for elongation, with the extent of elongation dependent on local concentrations of actin monomers and regulatory factors.

To test these predictions, we have studied the kinetics of actin assembly using pyrene-labeled actin in a fluorescence assay (39). We find that highly purified *D. discoideum* plasma membranes do nucleate actin assembly. Membrane-induced actin nuclei appear to have both ends free and the dependence of polymerization lag time on actin concentration is most consistent with a nucleus size of three. Nucleation activity is mediated by integral membrane proteins and requires an intact membrane bilayer. Although detergent-solubilized membranes are unable to nucleate actin assembly, activity can be completely reconstituted by dialysis or dilution of detergent extracts containing a complete complement of membrane proteins. By contrast, no detectable nucleation activity is recovered from detergent extracts that have been depleted of ponticulin by chromatography on a column containing antibody specific for this protein. These results indicate that ponticulin is required for the actin nucleation activity of plasma membranes in vitro and suggest that this protein may play a role in vivo in the initiation of actin polymerization at the cytoplasmic surfaces of plasma membranes during motile processes.

Materials and Methods

Chemicals

OG, phalloidin, and ATP were purchased from Boehringer Mannheim Biochemicals (Indianapolis, IN). NEM, DTT, BSA, CD, dimethylformamide, L-α-dipalmitoylphosphatidylcholine, and protein A-Sepharose were procured from Sigma Chemical Co. (St. Louis, MO). Acrylamide and SDS were supplied by Bio-Rad Laboratories (Richmond, CA). *N*-(1-pyrenyl)-iodoacetamide was from Molecular Probes Inc. (Eugene, OR). Sephadex G-25 and Sephadex G-150 were purchased from Pharmacia Fine Chemicals (Piscataway, NJ). Dimethylsuberimidate hydrochloride was from Pierce Chemical Co. (Rockford, IL). All other chemicals were reagent grade.

Proteins

Actin, isolated from rabbit skeletal muscle according to Spudich and Watt (64) was column-purified (46) on Sephadex G-150 in 0.2 mM $CaCl_2$, 1 mM ATP, 1 mM DTT, 2 mM Tris-HCl, pH 8.0 (buffer A), and stored in the G-form by dialysis against the same buffer. After 2 wk, the actin was cycled by polymerization and depolymerization, used for an additional two wk, and then discarded. Rabbit plasma gelsolin was prepared using a protocol graciously provided by Dr. C. Frieden (C. Frieden, unpublished observations).

Protein concentrations were determined in the presence of 1% SDS by the procedure of Lowry (42) with BSA as the standard. G-actin concentrations also were measured spectrophotometrically by using a value of $\epsilon^{1\ mg/ml} = 0.62$ at 290 nm (34) and a molecular mass of 43,000.

Actin Labeling

Pyrene actin was prepared according to the procedure of Kouyama and Mihashi (39) as modified by Cooper et al. (16). Briefly, gel-filtered actin (1 mg/ml) was dialyzed against 0.1 M $CaCl_2$, 0.2 mM ATP, 1 mM $NaHCO_3$, pH 7.6, and then polymerized by the addition of $MgCl_2$ to 2 mM and KCl to 0.1 M. Polymerized actin was mixed with a 7.5 molar excess of *N*-(1-pyrenyl)-iodoacetamide, which was initially dissolved in dimethylformamide. The final concentration of dimethylformamide in the reaction was <0.1%. The reaction mixture was gently rotated in the dark for 24 h at room temperature. The F-actin was pelleted by centrifugation at 180,000 *g* for 2 h (50 Ti rotor; Beckman Instruments, Inc., Palo Alto, CA) at 4°C, dissolved in buffer A, and dialyzed for at least 2 d against the same buffer. The depolymerized-labeled actin was clarified at 180,000 *g* for 30 min at 4°C and was separated from the unreacted dye by desalting on a Sephadex G-25 column in buffer A. Monomeric pyrene actin was prepared by chromatography on a Sephadex G-150 column equilibrated with buffer A. Actin typically was labeled to an extent of 0.7–0.9 mol/mol actin, as measured by using a molar extinction coefficient of $2.2 \times 10^4\ M^{-1}\ cm^{-1}$ at 344 nm for the protein-dye complex (39) corrected for the absorbance of native actin at 290 nm (16). Pyrene actin was stored in the same manner as unlabeled actin. Column-purified pyrene actin was diluted with column-purified unlabeled G-actin to form a 10% labeled mixture.

The critical concentration of the 10% labeled mixture was determined by measuring the fluorescence increase upon polymerization of different concentrations (0.1–12 μM) of pyrene actin (14). The critical concentration

also was determined by polymerizing the actin (400 μl, in triplicates) at 25°C for 2 h, pelleting F-actin in an airfuge (Beckman Instruments, Inc., 180,000 *g*, 20 min, 25°C), and measuring the protein concentration in the supernatant (67). With both techniques, the critical concentration was 0.2–0.3 μM, a concentration in agreement with published values (6, 16, 39, 67, 71).

Plasma Membranes

Highly purified plasma membranes, used in all the experiments described here, were prepared from log-phase amebae by the concanavalin A-stabilization, Triton-extraction method described by Luna et al. (44). Membranes containing residual endogenous actin were prepared by the same procedure except that cytoskeletal components were removed by dialysis for only 16–18 h instead of 2–3 d (58).

Membrane Extractions

Plasma membranes were extracted with 0.1 N NaOH, 1 mM DTT, pH 12.5, at 0–4°C for a total of 30 min, including centrifugation (44). The extraction mixture was sonicated with a single 5-s burst from a sonifier (model 200; Branson Sonic Power Co., Danbury, CT), and the membranes were pelleted by centrifugation at 27,900 *g* for 20 min at 4°C. The pellet containing the NaOH-extracted membranes was immediately resuspended and washed with 20 mM sodium phosphate, pH 6.8. Approximately 30% of the protein was recovered.

Heat-denatured membranes, proteolytically-digested membranes and *D. discoideum* lipid vesicles were prepared from purified plasma membranes according to published procedures (43). Organic solvent extractable phosphorus was measured as an estimate of phospholipid phosphorus (43). Briefly, plasma membranes, proteolyzed membranes, proteolysis control membranes, and lipid vesicles from *D. discoideum* plasma membranes (200–400 μl aliquots of each) were extracted with water-methanol-chloroform (5), and the chloroform layers were assayed for total phosphorus (2) using L-α-dipalmitoylphosphatidylcholine as a standard.

Periodate Oxidation

Periodate oxidation to remove or alter carbohydrate residues (21) was performed as described (74). NaOH-extracted plasma membranes at ~0.6 mg/ml were incubated in the dark for 12 h at 0°C with 50 mM $NaIO_4$, 10 mM sodium phosphate, pH 6.0. The reaction was stopped by the addition of ethylene glycol to a final concentration of 1% (vol/vol). After a further 30-min incubation on ice, membranes were diluted fivefold with 20 mM sodium phosphate, pH 6.8, and collected by centrifugation at 25,000 *g* for 40 min. The pellet was resuspended and washed twice in 20 mM sodium phosphate, pH 6.8. Control membranes were treated identically, except that $NaIO_4$ was omitted. About 80% of the protein was recovered from periodate-treated and control membranes.

Reduction and Alkylation of Membranes

Plasma membranes were treated with DTT and NEM as described (75). Briefly, plasma membranes at ~0.8 mg/ml were incubated at 37°C for 30 min in 50 mM DTT, 100 mM Tris-HCl, pH 7.5. Membranes were pelleted at 25,300 *g* for 20 min at 4°C and were washed twice in 200 mM Tris-HCl, pH 7.5. The pellet was resuspended with an equal volume of 100 mM NEM, 200 mM TRis-HCl, pH 7.5, and incubated for 30 min at 37°C. Alkylated membranes then were pelleted and washed with 20 mM sodium phosphate, pH 6.8. The final pellet, containing 75% of the initial membrane protein, was resuspended to 1 mg/ml with 20 mM sodium phosphate, pH 6.8.

Actin Seeds

A stock of actin seeds was made according to published procedure (28). Briefly, actin (25 μM) in buffer A was allowed to polymerize at 25°C for 24 h in the presence of 10 mM KCl, 10 μM $MgCl_2$, 25 μM phalloidin, and the mixture was stored at 0–4°C. Immediately before use, a portion of the stock was diluted 10-fold with buffer A and sonicated with two 30-sec bursts. As required, aliquots from the sonicated mixture were added directly into the polymerization assay mixture.

Fluorescence Measurements

Fluorescence was measured in an LS-3 fluorimeter (Perkin-Elmer Corp., Pomona, CA). Excitation and emission wavelengths for pyrene actin were set at 365 and 407 nm, respectively (39). To minimize photobleaching, the actin samples were only intermittently exposed to the exciting light. Polymerization assays were performed by adding pyrene actin (from a stock solution of 11–15 μM) to the sample in polymerization buffer (0.1 M KCl, 2 mM $MgCl_2$, 1 mM ATP, 25 mM imidazole, pH 7.0, final concentration). The final concentration of pyrene actin in the assays was 3 μM unless stated otherwise. To prevent membrane sedimentation and to reduce light scattering, plasma membranes were sonicated with a sonifier (Branson Sonic Power Co.) for a total of 6 min in 20-s bursts immediately before inclusion in the assay. Solutions were mixed quickly in a final volume of 0.5 ml and the fluorescence at 25°C was measured. The pyrene actin fluorescence was normalized from 0–10 and plotted versus time (16), with 10 being the fluorescence value of each sample after 24 h of polymerization unless stated otherwise.

Two procedures were used to prepare samples for the measurement of the depolymerization time course of actin. In the first procedure, duplicate samples of 20% labeled pyrene actin (3 μM, 130 μg/ml) and gelsolin (~0.06 μM, 6 μg/ml) were mixed in polymerization buffer containing 50 μM $CaCl_2$ and allowed to polymerize for 2 h at 25°C. Plasma membranes (25 μg/ml) then were added to one of the tubes and both samples were mixed and incubated at 25°C for 22 h. In the second procedure, the plasma membranes and actin were incubated for 2 h at 25°C before the subsequent addition of gelsolin (3, 6, or 12 μg/ml) and equilibration at 25°C for 22 h. To measure depolymerization, aliquots from each sample were diluted 50-fold into a cuvette containing polymerization buffer and 21 μM $CaCl_2$ (final concentration), and the fluorescence change was measured. As controls, aliquots also were diluted into polymerization buffer containing 5 μM phalloidin and 21 μM $CaCl_2$.

The log of the rate of the slow phase of actin polymerization versus the log of actin concentration was determined and plotted as described in Cooper et al. (15). The rate of the slow phase of actin polymerization is defined as the inverse of the delay time ($1/t_D$) before the approximately linear increase in pyrene actin fluorescence begins. For most experiments, actin was activated by preincubation for 5 min at 0°C in 250 μM $MgCl_2$, 3–15 μM $CaCl_2$, 1 mM ATP, 1 mM DTT, 2 mM Tris-HCl, pH 8.0. In one experiment, actin was activated by an overnight dialysis at 0°C against 250 μM $MgCl_2$ in buffer A. Both treatments favor the formation of activated, Mg^{++}-containing actin without supporting actin polymerization (24, 50), although transient oligomers of Mg^{++}-activated actin may be present (48, 50). Polymerization of activated or unactivated actin (0.5–3.0 μM) was monitored in the presence of polymerization buffer containing 20 μg/ml membranes and 100 μM $CaCl_2$. The increase in the fluorescence for each actin concentration was normalized and plotted versus time. Delay time was determined for each concentration of actin by measuring the x-intercept of a tangent drawn through the inflection point of the curve. The log $[1/t_D]$ was plotted against the log (actin concentration), and the slopes for each plot were determined by regression analysis using Cricket Graph and Statworks software.

PAGE and Protein Blotting

10–20% linear gradient polyacrylamide SDS slab gels were prepared and run according to the method of Laemmli (41). Radiolabeled proteins were denatured in sample buffer (1% SDS, 10% sucrose, 1 mM EDTA, 10 mM Tris-HCl, 0.1% bromophenol blue, 32 mM DTT, pH 8.0). Samples for immunoblotting were denatured in sample buffer without DTT. Radioactive gels were dried onto filter paper. Kodak XAR-5 film was exposed to the dried gels at room temperature (18–22°C). Molecular mass determinations were based on the molecular masses of Bethesda Research Laboratories prestained standards (69).

Nitrocellulose blots were prepared (68) by transferring electrophoretically separated proteins onto nitrocellulose (BA85, 0.45 μM pore size; Schleicher & Schuell, Inc., Keene, NH), blocking with 1% defatted milk, and fixing as previously described (75). Glutaraldehyde-fixed blots were incubated with 20 μg/ml IgG in 150 mM NaCl, 5 mM EDTA, 0.25% (wt/vol) gelatin, 0.05% Tween 20, 50 mM Tris-HCl, pH 7.4 (blotting buffer), for 2 h at room temperature, and then rinsed with blotting buffer. Blots were incubated with 200,000 cpm/ml of [^{125}I]protein-A (ICN Biomedicals Inc., Irvine, CA) in blotting buffer for 1 h at room temperature (8). Blots then were washed three times with blotting buffer, air-dried, and exposed to Kodak XAR-5 film at −80°C in the presence of Lightning Plus intensifying screen (Cronex; DuPont Co., Wilmington, DE).

Immunological Methods

Anti-$NaIO_4$-PM IgG, an antiserum raised against $NaIO_4$-treated NaOH-

extracted plasma membranes, was adsorbed exhaustively against glutaraldehyde-fixed, log-phase *D. discoideum* cells (74). Preimmune anti-$NaIO_4$-PM IgG was adsorbed similarly as a control.

Preparation of IgG-Protein A Matrix

Antibody-protein A matrices were made essentially as described (29, 57). Protein A-Sepharose (250 mg) was hydrated for 12 h at 4°C in PBS, pH 7.2, and washed with 50 ml of 0.1 M borate buffer, pH 8.2. The washed beads (bed volume ~1 ml) were mixed gently with 12 mg adsorbed anti-$NaIO_4$-PM IgG or adsorbed preimmune IgG for 30 min at room temperature. Unbound IgG was collected and the IgG-protein A beads were washed first with 10 ml of 0.1 M borate buffer, pH 8.2, and then with 10 ml of 0.2 M triethanolamine-HCl, pH 8.2. Washed beads were mixed gently for 45 min at room temperature with 20 ml of freshly prepared 20 mM dimethylsuberimidate hydrochloride, 0.2 M triethanolamine-HCl, pH 8.2. The beads were separated from the unreacted reagent by centrifugation at 500 *g* for 2 min. After blocking unreacted sites for 5 min at room temperature with 20 ml of 20 mM ethanolamine-HCl, pH 8.2, the IgG-protein A beads were washed three times with 10 ml of 20 mM sodium phosphate, pH 7.0, and stored at 4°C in the presence of 0.02% sodium azide.

IgG-Protein A-Sepharose Chromatography

IgG-protein A-Sepharose columns (0.2 ml bed vol) were preequilibrated with 10 column vol of 1% OG, 20 mM sodium phosphate, pH 7.0. Plasma membranes (200 μg), solubilized at 0.5 mg/ml in 3% OG, 50 mM KCl, 20 mM Tris-acetate, pH 7.0, for 10 min at 20–22°C, were clarified by centrifugation at 180,000 *g* for 30 min, and mixed gently with each IgG-protein A column for 1 h at room temperature. This ratio of column matrix to plasma membrane protein was determined in initial experiments to be about twice the minimum ratio required to bind all detectable plasma membrane ponticulin. Unbound proteins (run through fractions) were collected and the columns were washed with 10 column volumes each of 1 mg/ml BSA, 1% OG, PBS, pH 7.2, and 1 mg/ml BSA, 2% OG, 20 mM sodium phosphate, pH 7.0. Low affinity antigens were eluted with one column volume of 1.0 M guanidium chloride, 1% OG, 20 mM sodium phosphate, pH 7.0. High affinity antigens were eluted by mixing the IgG beads containing bound antigen with an equal volume of 4.5 M $MgCl_2$, 1 mg/ml BSA, 2% OG, 20 mM sodium phosphate, pH 7.0, for 30 min at room temperature and collecting the unbound proteins. The elution of high affinity antigens was repeated. The high affinity eluates were combined and desalted on Sephadex G-25 equilibrated with 2% OG, 1 mg/ml BSA, 20 mM sodium phosphate, pH 7.0.

Results

Membranes Accelerate Actin Assembly

The rate of actin polymerization was measured with a well-characterized, sensitive fluorescence assay employing pyrene actin (16, 39). This assay, which does not involve shearing the sample, is sensitive only to the polymer weight concentration and not to the distribution of filament lengths (16). In agreement with previous reports (for review, see references 14, 15, 28), Fig. 1 *A* (*open circles*) shows that the onset of actin polymerization is characterized by a delay, or lag phase. As originally proposed by Oosawa and Kasai (52), this lag results from the relatively slow processes of monomer activation and spontaneous nucleation that must occur before filament assembly and elongation can proceed (15, 25, 28, 72). After the lag, additional time is required before polymerization reaches a maximal rate (data not shown). *D. discoideum* plasma membranes dramatically decrease the polymerization lag time and increase the maximal rate of polymer formation (Fig. 1 *A*). At the actin concentration of 3 μM used here, the final extent of actin polymerization is not measurably affected by the addition of membranes (data not shown).

The membrane-induced increase in the maximal rate is linear with increasing membrane protein concentrations up to ~20 μg/ml (Fig. 1 *B*). At membrane concentrations above 20 μg/ml, the rate increases in a nonlinear manner, probably because of light scattering and viscosity effects (44). The rate of polymerization as a function of membrane protein concentration is 0.013 ± 0.001 $min^{-1} \cdot (\mu g/ml)^{-1}$ ($n = 3$ experiments), a value that is only 53.5-fold lower than the slope of 0.700 $min^{-1} \cdot (\mu g/ml)^{-1}$ obtained from a similar analysis of the nucleation activity of purified plasma gelsolin (data not shown), a well-characterized actin-nucleating protein (for review, see references 65, 76). This result suggests that the membrane-associated nucleating factor(s) comprise(s) as much as 2% of the total membrane protein and, thus, is a major membrane component.

Although the lag phase at the onset of polymerization is reduced in the presence of membranes, it is not eliminated (Fig. 1 and 2). Also, the additional time required to achieve the maximal rate is reduced, but not eliminated, in the presence of membranes. In both these respects, actin assembly in the presence of membranes is unlike the essentially immediate linear increase in actin polymerization observed

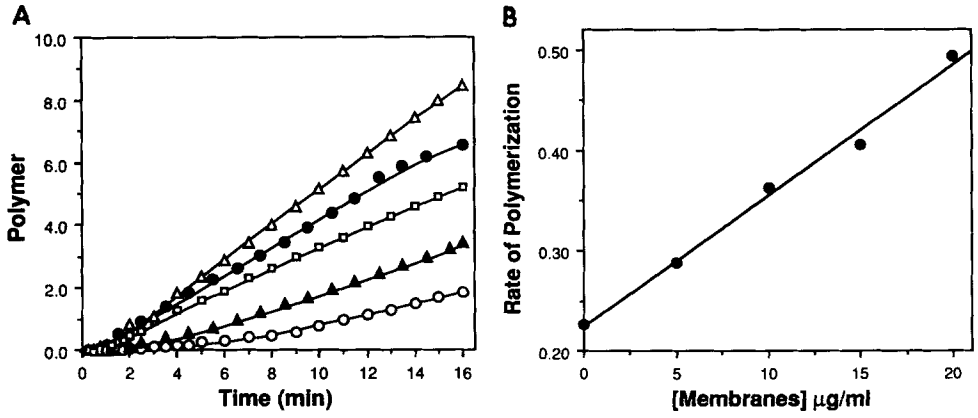

Figure 1. D. discoideum plasma membranes accelerate actin polymerization. (*A*) Polymerization kinetics as a function of membrane protein concentration. Pyrene actin at a final concentration of 3 μM was added to membranes in polymerization buffer. Fluorescence signal in normalized units is plotted versus time. Membrane protein concentrations in μg/ml are 5 (▲), 10 (□), 15 (●), and 20 (△). Control shows polymerization of actin alone (○). (*B*) Maximal rates of polymerization (from the slopes of the curves in *A*) versus membrane protein concentration. The slope of the line shown is 0.013 min^{-1} ($\mu g/ml$ protein)$^{-1}$ and the correlation coefficient (R^2) is 0.992.

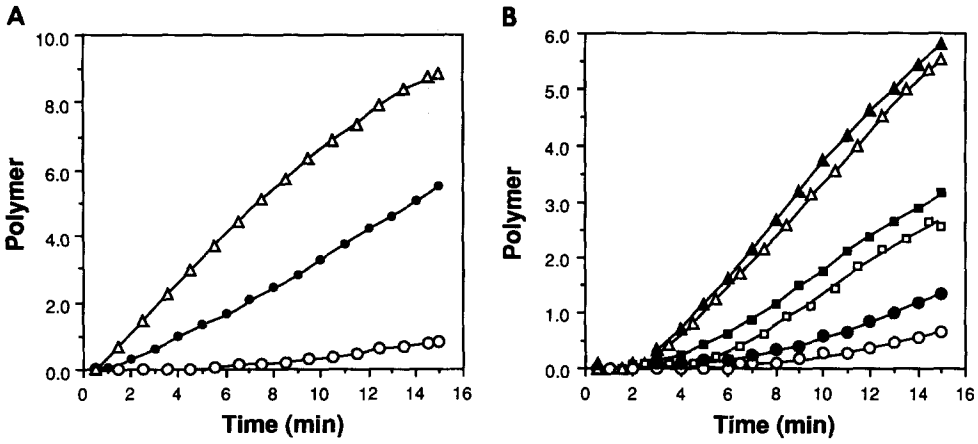

Figure 2. Plasma membranes reduce, but do not abolish, the delay time for actin polymerization. (*A*) Polymerization rate in the presence of 20 μg/ml highly purified plasma membranes (●) or 20 μg/ml prepolymerized actin seeds (△). Control shows polymerization of 3.0 μM actin alone (○). (*B*) Membranes accelerate the polymerization of both magnesium ion-activated and unactivated actin. Pyrene-actin in buffer A (*open symbols*) and pyrene actin activated by a 5-min preincubation at 0°C with 250 μM $MgCl_2$ (*closed symbols*) were polymerized by the addition of polymerization buffer and 10 μg/ml (*squares*) or 20 μg/ml (*triangles*) plasma membranes. Controls show polymerization of actin in the absence of membranes (*circles*). The final concentration of $MgCl_2$ was 2 mM in all cases.

in the presence of prepolymerized actin seeds (Fig. 2 *A*) (14, 15, 28). These observations suggest that plasma membranes potentiate either an initial, salt-induced conformational change in actin monomers (activation) or the subsequent association of activated monomers into oligomers (nucleation), which then rapidly elongate by further addition of monomers.

Plasma Membranes Potentiate the Nucleation Step of Actin Polymerization

Several experiments indicate that actin nucleation is the primary step that is accelerated by the presence of plasma membranes. First, membrane-induced acceleration of actin polymerization appears not to be due solely to an effect on the activation step. In a comparison of time courses of polymerization for preactivated actin versus actin activated in the assay in the presence of membranes, we found that membranes reduced the lag phase and accelerated actin polymerization regardless of whether or not the actin was preactivated (Fig. 2 *B*). This result indicates that the effect of membranes on actin assembly is not limited to an effect on monomer activation. However, the minimal difference between delay times for preactivated and assay-activated actin at higher membrane protein concentrations (Fig. 2 *B*, *triangles*) suggests that an effect of membranes on monomer activation cannot be ruled out. Furthermore, actin activation appears to be a prerequisite for membrane-mediated actin assembly as no membrane-induced actin polymerization is observed in the absence of salt (data not shown) (58).

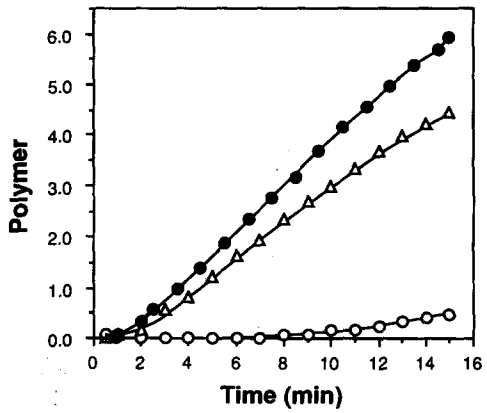

Figure 3. Acceleration of actin polymerization is not dependent on residual membrane-associated actin. Polymerization rate in the presence of highly purified plasma membranes without detectable (≤0.06%) residual actin (●) and plasma membranes that still have residual (≥0.5%) bound actin (△). Control shows polymerization of 3.0 μM actin alone (○).

Control experiments also eliminate the possibility that the actin assembly activity of *D. discoideum* plasma membranes is the result of elongation from preexisting, membrane-associated actin nuclei. First, the highly purified plasma membranes employed in these assays contain no detectable residual actin, as measured by an immunoblot assay with an estimated detection limit of 0.06% of the membrane protein (58). Second, membranes stripped of essentially all peripheral proteins with sodium hydroxide showed actin assembly activities comparable to those of unextracted plasma membranes (see below). Third, as mentioned above, elongation from actin seeds exhibits an initial linear time course that is distinct from the sigmoidal polymerization curves observed in the presence of plasma membranes (Fig. 2, *A* and *B*). Finally, membranes containing ≥0.5% of their mass as residual actin; i.e., with 5% or more of the available actin-binding sites occupied by endogenous actin, assembled actin at rates close to those mediated by membranes containing at least an order of magnitude less actin (Fig. 3). In fact, plasma membranes containing appreciable amounts of bound *Dictyostelium* actin reproducibly exhibited a slightly lower actin assembly activity than membranes without detectable actin. Because membranes preincubated with subcritical concentrations of purified rabbit actin do exhibit enhanced actin-nucleating activity (data not shown), we conclude that the residual endogenous actin either is blocked by endogenous capping factors or is inaccessible, perhaps trapped inside vesicles. In conclusion, elongation, like activation, appears not to be the principle step in actin assembly potentiated by membranes, leaving nucleation as the step most likely to be affected.

Membrane-mediated acceleration of the nucleation step is supported by a quantitative analysis of the relationship be-

Table I. Slopes of Log Rate vs. Log Actin Concentration*

Experiment	Actin Activated in Assay		Preactivated Actin	
	Slope	R^2	Slope	R^2
1	0.88	0.98	2.05	1.00
2	1.47	0.64	1.53	0.95
3	1.78	0.94	2.74	0.96
4	0.94	0.71	1.67	0.98
(Mean ± SEM:	1.27 ± 0.43‡		2.00 ± 0.54‡)	

* The rate is the inverse of the delay time before the onset of polymerization. Rates for unactivated and preactivated pyrene-labeled actin (0.5–3.0 μM) in the presence of plasma membranes (20 μg/ml) were determined as described in Materials and Methods. In experiments 1–3, actin was activated by a 5-min incubation with 250 μM $MgCl_2$; for experiment 4, actin was dialyzed overnight against 250 μM $MgCl_2$ in buffer A. Measured delay times ranged between ~0.5 min (3.0 μM preactivated actin) and ~8.8 min (0.8 μM assay-activated actin). The dependence of log rate on log actin concentration was determined by regression analysis of each of four independently obtained data sets. Both regression coefficients (slopes) and correlation coefficients of the lines (R^2) are presented.

‡ Means are significantly different ($P = 0.056$, paired t test).

tween delay time and actin concentration in assays containing plasma membranes (Table I). The slope of log [$1/t_D$] (a measure of the rate of the slow phase of actin polymerization) versus log [total actin] is 1.27 ± 0.43 for actin activated during the fluorescence assay in the presence of *D. discoideum* plasma membranes. This result is comparable to the values of 1.0–1.3 observed in similar experiments with actin activated by Mg^{++} in polymerization assays in the absence of other proteins (15). This result also is consistent with computer models in which a first-order process, such as the conformational change associated with monomer activation, is a rate-limiting step (15). By contrast, in experiments with actin preactivated with 250 μM $MgCl_2$ before inclusion in the assay (24), plots of log [$1/t_D$] versus log [total actin] exhibit slopes of 2.00 ± 0.54 in the presence of membranes (Table I). These slopes are similar to the slopes of 1.9–2.5 reported for actin polymerized in Ca^{++} (no Mg^{++}), a condition under which activation does not occur and nucleation is the slow initial step (15). Furthermore, a theoretical model in which nucleation is the rate-limiting step predicts a slope of 2.0 for a nucleus size of three monomers (Table III in reference 15). Slopes of 1.5 and 2.5 are predicted for nuclei containing two and four monomers, respectively. Therefore, our experimental observations are consistent with a rate-limiting step during polymerization that involves an actin nucleus of 3 ± 1 monomers.

Membrane-induced Actin Nuclei Have both Ends Free

To determine whether the fast-polymerizing "barbed" ends of membrane-induced actin nuclei are available for the addition of pyrene actin monomers, polymerization assays were performed in the presence of CD. CD binds and blocks the barbed ends of actin filaments, nucleates actin assembly by binding actin dimers, and increases the critical concentration for filament assembly (for review, see reference 13). As shown in Fig. 4 *A*, 0.5 μM CD dramatically reduces the final extent of polymerization in solutions containing 3.0 μM actin. Interestingly, membranes partially reverse the CD-induced reduction, suggesting that the effect of membranes on actin polymerization is distinct from the action of CD. Another effect of CD is the inhibition of the membrane-mediated acceleration of polymerization. This result suggests that, without CD, the barbed ends of actin filaments assembled in the presence of membranes are free to elongate. In the presence of CD, samples with and without membranes (*closed and open triangles*) exhibit approximately the same initial rate of filament assembly. This rate is only ~30% of the rate observed for actin plus membranes in the absence of CD (*closed circles*), but is greater than the rate of polymerization of the actin control (*open circles*), implying that elongation occurs from the pointed ends of CD-nucleated filaments in both the presence and absence of membranes.

Depolymerization studies support the idea that the pointed ends of actin filaments are not blocked by membranes. When added to G-actin in the presence of micromolar calcium ions, gelsolin forms a complex with two actin monomers which

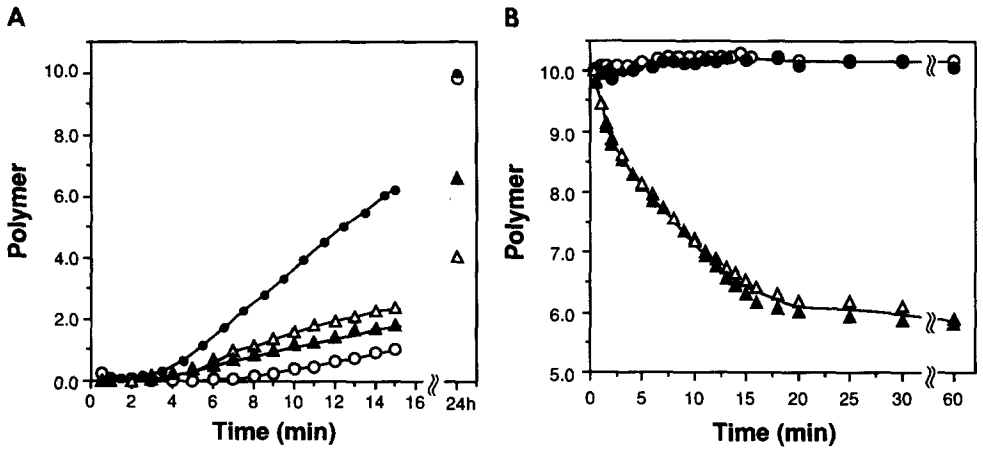

Figure 4. Membrane-nucleated actin filaments have both ends free. (*A*) The rate of membrane-induced actin polymerization is decreased by CD. Pyrene actin at 130 μg/ml (3 μM) was polymerized in the presence (*triangles*) and absence (*circles*) of 0.5 μM CD and in the presence (*solid symbols*) and absence (*open symbols*) of 20 μg/ml of *D. discoideum* plasma membranes. The final fluorescence at 24 h of actin alone was taken as 10 and all data sets were normalized to this value. (*B*) Time course of depolymerization of actin in the presence of plasma membranes. Actin (3 μM, 20% labeled) and gelsolin (0.06 μM) were mixed for 2 h in polymerization buffer containing 50 μM $CaCl_2$. Polymerization was continued for another 22 h in the presence (*solid symbols*) or absence (*open symbols*) of plasma membranes (25 μg/ml), an amount sufficient to bind 0.06–0.10 μM actin. An aliquot from each mixture was diluted 50-fold and the rate of decrease in fluorescence caused by depolymerization was monitored (*triangles*). Controls (*circles*) show the fluorescence change upon dilution in the presence of phalloidin (5 μM). Initial fluorescence of the phalloidin-containing sample was taken as 10 and all data were normalized to this value.

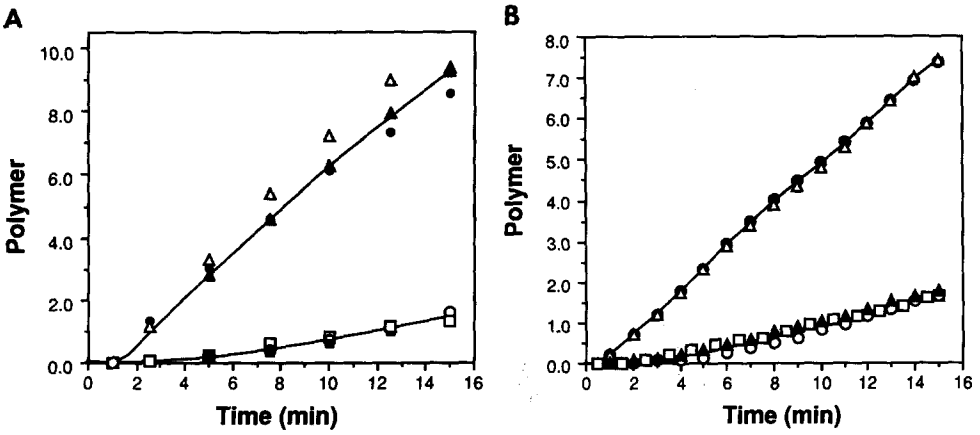

Figure 5. Actin nucleation activity is mediated by integral membrane proteins. (*A*) Pyrene actin was polymerized in the absence (○) and in the presence of untreated plasma membranes (●); NaOH-extracted membranes (▲); periodate treated membranes (△); heat-denatured membranes (■); or membranes treated with DTT and NEM (□). Each assay with membranes contained 20 μg/ml membrane protein. (*B*) Pyrene actin was polymerized in the absence (○) and in the presence (●) of untreated plasma membranes; proteolyzed membranes (▲); proteolysis control membranes (△); or vesicles reconstituted from *D. discoideum* lipids (□). Each assay with membranes contained ~14 nmol phospholipid-equivalent.

then nucleates actin filament assembly (for review, see references 65, 76). Gelsolin remains tightly bound to the barbed end of the filaments, preventing further elongation from this end. In the presence of tightly bound gelsolin, actin depolymerization occurs solely from the pointed ends of the filaments (17, 20, 36). As shown in Fig. 4 *B*, the depolymerization rates of gelsolin-capped pyrene actin are identical in the presence and absence of membranes, clearly indicating that membranes do not block the pointed ends. As expected from the observation that actin binds independently and concurrently to gelsolin and *D. discoideum* plasma membranes (58), essentially identical depolymerization curves also are obtained when actin filaments are assembled in the presence of membranes before the barbed ends are capped with gelsolin (data not shown). In conjunction with the polymerization studies presented above, these results provide strong evidence that membrane-induced actin nuclei have both their barbed and pointed ends free.

Integral Membrane Proteins Mediate the Actin Nucleation Activity

Actin nucleation activity, like the previously-described actin-binding and assembly activities of *D. discoideum* membranes (43, 44, 58), appears to be mediated by integral membrane proteins. Nucleation activity persists after extraction of peripheral proteins with chaotropic agents, but is destroyed upon proteolysis, heat-treatment, or alkylation of membranes (Fig. 5, *A* and *B*). Control membranes, which are taken through the same steps as the proteolyzed membranes, but in the absence of protease, retain full activity (Fig. 5 *B*). Also, the removal or alteration of carbohydrate moieties by periodate treatment of membranes does not affect the membrane-mediated increase in the initial rate of actin polymerization (Fig. 5 *A*). Finally, vesicles reconstituted from *D. discoideum* lipids exhibit no actin nucleating activity (Fig. 5 *B*).

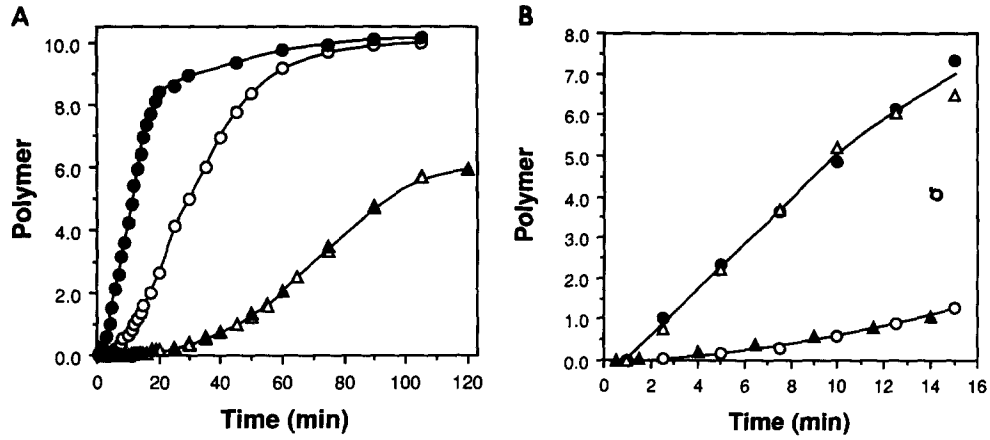

Figure 6. Detergent solubilization reversibly disrupts the membrane-mediated actin nucleation activity. (*A*) Detergent solubilization of membranes eliminates actin nucleation activity. Polymerization of pyrene actin was monitored in the presence (*triangles*) and absence (*circles*) of 2% octylglucoside and in the presence (*solid symbols*) and absence (*open symbols*) of 20 μg/ml plasma membranes. All data were normalized to the fluorescence value of actin alone at 24 h of polymerization. (*B*) Reconstitution of detergent-solubilized membranes restores actin nucleation activity. Plasma membranes (0.5 mg/ml) were solubilized in 3% octylglucoside and clarified at 180,000 *g*. The small pellet was resuspended in 200 μl of 20 mM sodium phosphate, pH 6.8. The supernatant was dialyzed against 0.5% octylglucoside, 20 mM sodium phosphate, pH 6.8, for 12 h at 4°C. Polymerization of pyrene actin was monitored in the presence of 20 μg/ml of untreated plasma membranes (●), a 23-fold dilution (to 20 μg/ml) of the octylglucoside-solubilized, dialyzed supernatant (△), or a sixfold dilution (to 20 μg/ml) of the octylglucoside pellet (▲). Control shows polymerization of pyrene actin alone (○). The final octylglucoside concentration in the polymerization assay was <0.02%. Data were normalized to the fluorescence after 24 h of polymerization that was the same for all samples.

Nucleation Activity Is Reversibly Disrupted by Detergent

Although *D. discoideum* lipids do not, by themselves, nucleate actin assembly, an intact lipid bilayer may be required for this process (Fig. 6). In the presence of 2% OG, a detergent concentration that disrupts the lipid bilayer and completely solubilizes plasma membrane proteins but supports the binding of solubilized membrane proteins to F-actin columns (73), no nucleation of actin assembly is observed (Fig. 6 *A*). In 2% OG, both the initial rate and the final extent of actin polymerization are independent of the presence of membranes and are reduced by ~40% (Fig. 6 *A*). Lowering the concentration of OG below its critical micelle concentration by dialysis or dilution restores nucleation activity (Fig. 6 *B*). Essentially all nucleation activity associated with the sonicated membrane vesicles, which are "scrambled" with respect to their initial membrane orientation (31), appears to be solubilized by OG and can be reconstituted after detergent dialysis or dilution.

Ponticulin Is Required for Nucleation Activity

Since both the actin-nucleation and actin-binding activities of plasma membranes appear to be mediated by integral membrane proteins and since ponticulin, an integral glycoprotein, is the major actin-binding protein in these membranes (74), we explored the possibility that ponticulin is involved in the nucleation of actin assembly. We used a column containing adsorbed anti-$NaIO_4$-PM IgG, an antibody directed predominantly against the cytoplasmic domain of ponticulin (74), to remove ponticulin from detergent-solubilized membrane extracts. Adsorbed anti-$NaIO_4$-PM IgG specifically recognizes ponticulin and a minor structurally-related 15-kD protein, as visualized on immunoblots (Fig. 7 *A*, lane *1*) (75) and by immunoprecipitation of detergent-solubilized ^{125}I-labeled plasma membranes (data not shown) (74). Adsorbed preimmune IgG does not recognize any membrane protein by either method (74, 75). After chromatography of OG-solubilized membrane extracts on affinity columns, ponticulin is present in the run-through from the adsorbed preimmune IgG column (Fig. 7 *A*, lane *2*) but not in the run-through from the column containing adsorbed anti-$NaIO_4$-PM IgG (Fig. 7 *A*, lane *3*). The depletion of ponticulin in the latter fraction is because of retention by ponticulin-specific antibody (Fig. 7 *A*, lanes *4* and *5*).

SDS-gels of OG-solubilized, ^{125}I-labeled plasma membrane proteins (Fig. 7 *B*, lane *1*) show that, despite the specificity of the antibody, ponticulin is not the only protein

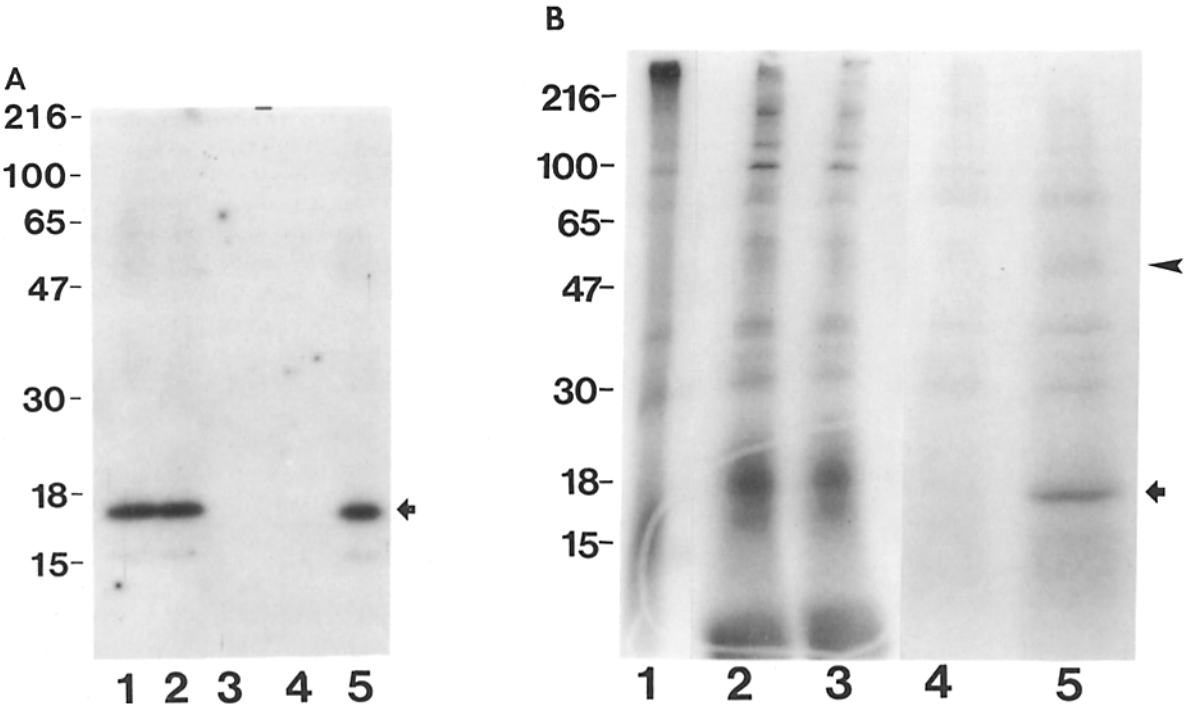

Figure 7. Proteins in fractions from IgG-Protein A Sepharose columns. (*A*) Autoradiograph of a nitrocellulose blot, stained with anti-$NaIO_4$-PM IgG and [^{125}I]protein A, containing: 10 μg of plasma membranes (lane *1*); 55 μl of the run-through fraction from the preimmune IgG column (lane *2*); 55 μl of the run-through fraction from the anti-$NaIO_4$-PM IgG column (lane *3*); 60 μl of desalted $MgCl_2$ eluate from the preimmune IgG column (lane *4*); and 60 μl of desalted $MgCl_2$ eluate from the anti-$NaIO_4$-PM IgG column (lane *5*). Samples were desalted as described in Materials and Methods. The nitrocellulose blot was exposed to film for 3 d. The arrow denotes the position of ponticulin. (*B*) Autoradiograph of a 10–20% polyacrylamide gel showing ^{125}I-labeled membrane proteins in IgG column fractions. Plasma membranes were radiolabeled with [^{125}I]Bolton Hunter reagent (74) and solubilized and chromatographed as described in Materials and Methods. Lanes contain: 10 μl of clarified OG solubilized membranes (lane *1*); 50 μl of the run-through fraction from the preimmune IgG column (lane *2*); 50 μl of the run-through fraction from the anti-$NaIO_4$-PM IgG column (lane *3*); 100 μl of desalted $MgCl_2$ eluate from the preimmune IgG column (lane *4*); and 100 μl of desalted $MgCl_2$ eluate from the anti-$NaIO_4$-PM IgG column (lane *5*). Samples were desalted as described in Materials and Methods. The dried gel was exposed to film for 2.5 d (lanes *1–3*) and for 3 wk (lanes *4–5*). The arrow denotes the position of ponticulin and the arrowhead denotes the position of the 50-kD polypeptide.

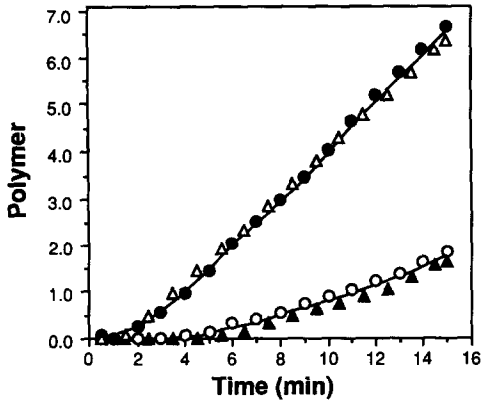

Figure 8. Removal of ponticulin from membrane extracts correlates with loss of actin nucleation activity. Polymerization of pyrene actin was monitored in the presence of 20 μg/ml of plasma membranes (●); a 25-fold dilution (20 μl) of the flow-through fraction from the anti-$NaIO_4$-PM IgG–protein A Sepharose column (▲); or a 25-fold dilution (20 μl) of the flow-through fraction from the preimmune IgG–protein A Sepharose column (△). Control shows polymerization of pyrene actin alone (○). The final octylglucoside concentration in the polymerization assay was 0.12%.

bound to columns containing adsorbed anti-$NaIO_4$-PM IgG (Fig. 7 *B*, lane *5*). First, in the absence of a carrier protein to block nonspecific sites on the column matrix (74), small and variable amounts of several major membrane proteins (Fig. 7 *B*, lanes *1–3*) bind to both the adsorbed preimmune and adsorbed anti-$NaIO_4$-PM IgG columns (Fig. 7 *B*, lanes *4* and *5*). More interestingly, a relatively minor 50-kD polypeptide specifically binds and elutes with ponticulin in the high-affinity fraction from the adsorbed anti-$NaIO_4$-PM IgG column (Fig. 7 *B*, lane *5*). As the 50-kD polypeptide is not recognized directly by this antibody on immunoblots (Fig. 7 *A*, lane *5*) or in immunoprecipitations (74), the presence of this protein on the adsorbed anti-$NaIO_4$-PM IgG column suggests that the 50-kD polypeptide may associate with ponticulin in detergent micelles.

After reconstitution in nucleation assays, essentially full actin nucleation activity is recovered in the preimmune column run-through (Fig. 8, *open triangles*), while the rate of actin polymerization falls to that of actin alone in the presence of run-through from the adsorbed anti-$NaIO_4$-PM IgG column (Fig. 8, *closed triangles*). Since ponticulin is the only major protein removed by the latter column (Fig. 7, *A* and *B*, lanes *5*) and is the only protein in this fraction that directly binds ^{125}I-labeled actin on nitrocellulose blots after SDS-gel electrophoresis (Chia, C., P. A. L. Hitt, and E. J. Luna, manuscript in preparation), ponticulin appears to be involved in the membrane-mediated nucleation of actin assembly. In initial attempts to reconstitute activity from the ponticulin-rich fraction eluted with 4.5 M $MgCl_2$ from the adsorbed anti-$NaIO_4$-PM IgG column (Fig. 7, *A* and *B*, lanes *5*), we have recovered only a small fraction of the expected actin nucleation activity. Apparently, the harsh conditions necessary to elute ponticulin from the antibody column destroy the nucleation activity and preclude reconstitution, either alone or after mixing with the run-through fraction from the adsorbed anti-$NaIO_4$-PM IgG column. Therefore, another approach is required to determine whether ponticulin nucleates actin assembly alone or in concert with other membrane components such as the 50-kD polypeptide.

Discussion

In this paper, we present evidence for an actin-nucleating activity associated with *D. discoideum* plasma membranes. These membranes both reduce the delay time before the onset of actin polymerization and increase the maximal rate of actin assembly (Fig. 1–4). Both these effects appear to require the salt-dependent activation of actin monomers, but activation is not the major step in the polymerization process potentiated by membranes (Fig. 2). A principal effect of membranes on the elongation step also is contraindicated (Fig. 3 and 5). Finally, log–log plots of the initial, slow rate of polymerization versus concentration of preactivated actin (Table I) are consistent with a theoretical model in which the rate-limiting step involves a nucleus of 3 ± 1 actin monomers (14). Thus, actin polymerization in the presence of membranes appears to involve the same fundamental sequence of events as that described for actin in solution (for review, see references 26, 54). Although quantitative effects on other steps in the polymerization process cannot be ruled out, membranes appear to affect primarily the rate(s) of a kinetic step(s) associated with nucleation. The present temporal resolution of our data does not permit us to distinguish between a membrane-induced acceleration of nucleus formation at the membrane surface and membrane-mediated stabilization of transient actin nuclei formed in solution.

The biochemical basis for the actin nucleation activity of *D. discoideum* plasma membranes appears to be the same as that responsible for high-affinity actin-membrane binding (43, 44, 58). Like actin binding to membranes, membrane-mediated actin nucleation persists after extraction of membranes with chaotropes, but is destroyed by membrane proteolysis, heat denaturation, or treatment with DTT and *N*-ethyl maleimide (NEM) (Fig. 5), indicating that integral membrane proteins are involved. In agreement with the previous observation that monovalent antibody fragments recognizing ponticulin inhibit 96% of actin-membrane binding in sedimentation assays (74), we find that the removal of ponticulin from detergent extracts abolishes the ability to reconstitute nucleation activity (Fig. 8). As the present procedure obviates the possibility of artifactual steric blocking by antibody fragments, it provides direct evidence that ponticulin, either with or without associated proteins, is required for essentially all the actin-nucleating activity, and perhaps also for essentially all actin-binding activity, of these membranes.

Assuming that essentially all the measured actin-nucleating activity of *D. discoideum* plasma membranes is caused by ponticulin, the specific activity of this protein is at least as high as that of plasma gelsolin. Defining nucleation activity as the slope of the maximal rate of polymerization versus molar concentration of nucleating protein, we find that the nucleation activity of plasma gelsolin is 60 min^{-1} μM^{-1}, given a molecular mass of 86 kD (40). Assuming that ponticulin constitutes 0.7% of the total membrane protein (74), that half of the total ponticulin is accessible at the exterior surfaces of the sealed membrane vesicles (31), and that each 17-kD monomer forms an active nucleation site, we calculate from the slope in Fig. 1 *B* that the nucleation activity of ponticulin is 63 min^{-1} μM^{-1}. This value, which is very close to the nucleation activity of plasma gelsolin, is a minimum estimate because elongation from membrane-induced nuclei, unlike gelsolin-actin complexes, can occur at both ends of the actin

filaments (Fig. 4). Also, as discussed below, it is likely that ponticulin must be at least dimeric to function as a nucleation site. Thus, ponticulin, a major membrane component, appears to have about the same, or higher, specific nucleation activity as gelsolin, a purified actin-nucleating protein. Although a requirement for a moderately-abundant protein such as the 50-kD polypeptide (Fig. 7 *B*) cannot be ruled out, this calculation indicates that it is very unlikely that a minor membrane protein, such as the 15-kD ponticulin-related polypeptide (Fig. 7 *A*), is primarily responsible for the observed membrane-mediated actin nucleation activity.

The nucleation activity of *D. discoideum* plasma membranes characterized in this paper differs in significant respects from the membrane-mediated actin nucleation described by other workers. In erythrocyte and baby hamster kidney cell membrane preparations, actin nuclei appear to be responsible for the enhanced polymerization of pyrene-labeled G-actin (37, 38, 53). Linear fluorescence increases occur immediately after mixing actin and membranes (38, 53), and extraction of membranes with actin-depolymerizing buffers reduces or eliminates subsequent actin-membrane association (12, 38, 70). In contrast, *D. discoideum* plasma membranes devoid of peripheral proteins, including actin, still nucleate actin assembly (Fig. 3. and 5 *A*) with an initial time course of polymerization distinctly different from that observed in the presence of actin seeds (Fig. 2). Although a similar activity has not yet been documented in other membranes, a 17-kD analogue of ponticulin has been found in human polymorphonuclear leukocyte plasma membranes (75), suggesting that ponticulin-mediated actin nucleation is present in other eukaryotic cells.

The observations reported here support the model for the assembly of actin filaments on plasma membranes proposed by Schwartz and Luna (59). This working model, based on geometric considerations and observations from equilibrium binding studies, predicts, first, that actin assembly at membranes should involve either the creation, or stabilization, of actin nuclei. Membrane-mediated acceleration of the nucleation step of filament assembly is confirmed by the kinetic experiments with pyrene actin detailed above. Second, the model requires that membrane-bound actin nuclei initially assemble with both barbed and pointed ends free. We have demonstrated that, in fact, actin nuclei assembled in the presence of membranes do have free barbed ends, at least until these ends are blocked with a capping factor, such as CD (Fig. 4 *A*) or gelsolin. The existence of free pointed ends on actin filaments associated with membranes is supported by both polymerization (Fig. 4 *A*) and depolymerization (Fig. 4 *B*) experiments conducted with filaments capped at their barbed ends. A third prediction of the model is that membrane-apposed actin filaments should be "untwisted" and perhaps short because of rotational strain. Although we have not yet tested this idea, it is interesting that short, gelsolin-capped actin filaments have been visualized in association with the cytoplasmic surfaces of macrophage membranes (33). A final, also untested prediction of the model is that actin-nucleating sites on membranes should consist of multiple actin-binding sites that are stably associated with each other and spaced about 5.4-nm apart, the approximate distance between adjacent subunits on the same side of an actin filament (for review, see reference 22). While this condition could be satisfied by the existence of multiple actin-binding domains in a single polypeptide, given the small size of ponticulin (the only actin-binding protein thus far implicated in this phenomenon), it is likely that either oligomers of ponticulin or complexes of ponticulin with other polypeptides are involved. Disruption of such an oligomeric complex by detergent could explain the dependence of nucleation activity on the integrity of the membrane bilayer (Fig. 6). Alternatively, the requirement for an intact bilayer may be because of the increased local concentration of ponticulin that accompanies the conversion of a three-dimensional micellar solution into a two-dimensional membrane (1, 18).

It will be especially important to ascertain whether structural changes in putative ponticulin-containing complexes correlate with the formation of new actin nucleation sites and/or increased actin polymerization during motile processes. At least theoretically, newly created membrane-associated actin filaments could act as a template for further recruitment of actin filaments through the lateral binding of actin-cross-linking (or bundling) proteins, which then nucleate more filaments. Depending upon the regulatory proteins involved, either an amorphous meshwork (such as those associated with pseudopod extension) or a structure with a high degree of local order (e.g., actin bundles in filopodia and microvilli) could result. In conjunction with the recent finding that microtubule-associated proteins in two-dimensional arrays provide a template for the assembly of new microtubules (60), our work suggests that lateral nucleation may be generally important for cytoskeletal assembly processes.

We thank Drs. Cathy Chia, Anne Hitt, Yu-Li Wang, Martin A. Schwartz, Alonzo Ross, and Mitchell Sanders for their helpful comments and critical suggestions on the manuscript. We are especially grateful to Martin Schwartz for suggesting that we compare the membrane-mediated nucleation activity with that of gelsolin.

This work was supported by National Institutes of Health grant GM33048 and American Cancer Society grant CD-387. This work also benefited from a Faculty Research Award (FRA-289), from the American Cancer Society to E. J. Luna, and from NCI Cancer Center Support (Core) Grant P30-12708-17 to the Worcester Foundation for Experimental Biology.

Received for publication 12 September 1989 and in revised form 20 November 1989.

References

1. Adam, G., and Delbrück. 1968. Reduction of dimensionality in biological diffusion processes. *In* Structural Chemistry and Molecular Biology. A. Rich and N. Davidson, editor. W. H. Freeman and Company, San Francisco. 198–215.
2. Ames, B. N. 1966. Assay of inorganic phosphate, total phosphate and phosphatases. *Methods Enzymol.* 8:115–118.
3. Bennett, H., and J. Condeelis. 1984. Decoration with myosin subfragment-1 disrupts contacts between microfilaments and the cell membrane in isolated *Dictyostelium* cortices. *J. Cell Biol.* 99:1434–1440.
4. Besterman, J. M., and R. B. Low. 1983. Endocytosis: a review of mechanisms and plasma membrane dynamics. *Biochem. J.* 210:1–13.
5. Bligh, E. G., and W. J. Dyer. 1959. A rapid method of total lipid extraction and purification. *Can. J. Biochem. Physiol.* 37:911–917.
6. Bonder, E. M., D. J. Fishkind, and M. S. Mooseker. 1983. Direct measurement of critical concentrations and assembly rate constants at the two ends of an actin filament. *Cell.* 34:491–501.
7. Brown, S. S., and A. S. Petzold. 1987. Using antibodies against *Dictyostelium* membranes to identify an actin-binding membrane protein. *J. Cell Biol.* 104:513–518.
8. Burnette, W. N. 1981. "Western blotting": electrophoretic transfer of proteins from sodium dodecyl sulfate-polyacrylamide gels to unmodified nitrocellulose and radiographic detection with antibody and radioiodinated Protein A. *Anal. Biochem.* 112:195–203.
9. Burridge, K., K. Fath, T. Kelly, G. Nuckolls, and C. Turner. 1988. Focal

adhesions: transmembrane junctions between the extracellular matrix and the cytoskeleton. *Annu. Rev. Cell Biol.* 4:487–525.
10. Carraway, K. L., and C. A. C. Carraway. 1989. Membrane-cytoskeleton interactions in animal cells. *Biochim. Biophys. Acta.* 988:147–171.
11. Carson, M., A. Weber, and S. H. Zigmond. 1986. An actin-nucleating activity in polymorphonuclear leukocytes is modulated by chemotactic peptides. *J. Cell Biol.* 103:2707–2714.
12. Cohen, C. M., P. L. Jackson, and D. Branton. 1978. Actin-membrane interactions: Association of G-actin with the red cell membrane. *J. Supramol. Struct.* 9:113–124.
13. Cooper, J. A. 1987. Effects of cytochalasin and phalloidin on actin. *J. Cell Biol.* 105:1473–1478.
14. Cooper, J. A., and T. D. Pollard. 1982. Methods to measure actin polymerization. *Methods Enzymol.* 85:182–210.
15. Cooper, J. A., E. L. Buhle Jr., S. B. Walker, T. Y. Tsong, and T. D. Pollard. 1983*a*. Kinetic evidence for a monomer activation step in actin polymerization. *Biochemistry.* 22:2193–2202.
16. Cooper, J. A., S. B. Walker, and T. D. Pollard. 1983. Pyrene actin: Documentation of the validity of a sensitive assay for actin polymerization. *J. Musc. Res. Cell Motil.* 4:253–262.
17. Coué, M., and E. D. Korn. 1985. Interaction of plasma gelsolin with G-actin and F-actin in the presence and absence of calcium ions. *J. Biol. Chem.* 260:15033–15041.
18. DeLisi, C. 1981. The effect of cell size and receptor density on ligand-receptor reaction rate constants. *Mol. Immunol.* 18:507–511.
19. Devreotes, P. N., and S. H. Zigmond. 1988. Chemotaxis in eucaryotic cells: a focus on leukocytes and *Dictyostelium*. *Annu. Rev. Cell Biol.* 4:649–686.
20. Doi, Y., and C. Frieden. 1984. Actin polymerization. The effect of brevin on filament size and rate of polymerization. *J. Biol. Chem.* 259:11868–11875.
21. Dyer, J. R. 1956. Use of periodate in biochemical analysis. *In* Methods of Biochemical Analysis. D. Glick, editor. Interscience Publishers, Inc., New York. 111–152.
22. Egelman, E. H. 1985. The structure of F-actin. *J. Musc. Res. Cell Motil.* 6:129–151.
23. Egelman, E. H., N. Francis, and D. J. DeRosier. 1982. F-actin is a helix with a random variable twist. *Nature (Lond.).* 298:131–135.
24. Frieden, C. 1982. The Mg^{++}-induced conformational change in rabbit skeletal muscle G-actin. *J. Biol. Chem.* 257:2882–2886.
25. Frieden, C. 1983. Polymerization of actin: Mechanism of the Mg^{2+}-induced process at pH 8 and 20°C. *Proc. Natl. Acad. Sci. USA.* 80:6513–6517.
26. Frieden, C. 1985. Actin and tubulin polymerization: The use of kinetic methods to determine mechanism. *Annu. Rev. Biophys. Biophys. Chem.* 14:189–210.
27. Geiger, B. 1983. Membrane-cytoskeleton interaction. *Biochim. Biophys. Acta.* 737:305–341.
28. Gershman, L. C., J. Newman, L. A. Selden, and J. E. Estes. 1984. Bound-cation exchange affects the lag phase in actin polymerization. *Biochemistry.* 23:2199–2203.
29. Gersten, D. M., and J. J. Marchalonis. 1978. A rapid, novel method for the solid-phase derivatization of IgG antibodies for immune-affinity chromatography. *J. Immunol. Methods.* 24:305–309.
30. Goodloe-Holland, C. M., and E. J. Luna. 1984. A membrane cytoskeleton from *Dictyostelium discoideum*. III. Plasma membrane vesicles bind predominantly to the sides of actin filaments. *J. Cell Biol.* 99:71–78.
31. Goodloe-Holland, C. M., and E. J. Luna. 1987. Purification and characterization of *Dictyostelium discoideum* plasma membranes. *Methods Cell Biol.* 28:103–128.
32. Hall, A. L., A. Schlein, and J. S. Condeelis. 1988. Relationship of pseudopod extension to chemotactic hormone-induced actin polymerization in amoeboid cells. *J. Cell Biochem.* 37:285–299.
33. Hartwig, J. H., K. A. Chambers, and T. P. Stossel. 1989. Association of gelsolin with actin filaments and cell membranes of macrophages and platelets. *J. Cell Biol.* 108:467–479.
34. Houk, T. W. J., and K. Ue. 1974. A measurement of actin concentration in solution: a comparison of methods. *Anal Biochem.* 62:66–74.
35. Ingalls, H. M., G. Barcelo, L. J. Wuestehube, and E. J. Luna. 1989. Developmental changes in protein composition and the actin-binding protein ponticulin in *Dictyostelium discoideum* plasma membranes purified by an improved method. *Differentiation.* 41:87–98.
36. Janmey, P. A., and T. P. Stossel. 1986. Kinetics of actin monomer exchange at the slow growing ends of actin filaments and their relation to the elongation of filaments shortened by gelsolin. *J. Musc. Res. Cell Motil.* 7:446–454.
37. Koffer, A., and M. Daridan. 1985. Actin-regulating activities in cultured BHK cells. *J. Cell Sci.* 75:239–257.
38. Koffer, A., and A. Edgar. 1989. Enhanced number of actin binding sites on plasma membranes of polyoma virus-transformed fibroblasts. *Biochim. Biophys. Acta.* 982:295–299.
39. Kouyama, T., and K. Mihashi. 1981. Fluorimetry study of N-(1-pyrenyl)iodoacetamide-labelled F-actin. *Eur. J. Biochem.* 114:33–38.
40. Kwiatkowski, D. J., T. P. Stossel, S. H. Orkin, J. E. Mole, H. R. Colten, and H. L. Yin. 1986. Plasma and cytoplasmic gelsolins are encoded by a single gene and contain a duplicated actin-binding domain. *Nature (Lond.).* 323:455–458.
41. Laemmli, U. K. 1970. Cleavage of structural proteins during the assembly of the head of bacteriophage T4. *Nature (Lond.).* 227:680–685.
42. Lowry, O. H., N. Rosebrough, A. L. Farr, and R. J. Randall. 1951. Protein measurement with the Folin phenol reagent. *J. Biol. Chem.* 193:265–275.
43. Luna, E. J., V. M. Fowler, J. Swanson, D. Branton, and D. L. Taylor. 1981. A membrane cytoskeleton from *Dictyostelium discoideum*. I. identification and partial characterization of an actin-binding activity. *J. Cell Biol.* 88:396–409.
44. Luna, E. J., C. M. Goodloe-Holland, and H. M. Ingalls. 1984. A membrane cytoskeleton from *Dictyostelium discoideum*. II. Integral proteins mediate the binding of plasma membranes to F-actin affinity beads. *J. Cell Biol.* 99:58–70.
45. Luna, E. J., L. J. Wuestehube, H. M. Ingalls, and C. P. Chia. 1989. The *Dictyostelium discoideum* plasma membrane: a model system for the study of actin-membrane interactions. *Adv. Cell Biol.* 3:1–33.
46. MacLean-Fletcher, S., and T. D. Pollard. 1980. Identification of a factor in conventional muscle actin preparations which inhibits actin filament self-association. *Biochem. Biophys. Res. Commun.* 96:18–27.
47. McRobbie, S. J. 1986. Chemotaxis and cell motility in the cellular slime molds. *CRC Crit. Rev. Microbiol.* 13:335–375.
48. Mozo-Villarias, A., and B. R. Ware. 1985. Actin oligomers below the critical concentration detected by fluorescence photobleaching recovery. *Biochemistry.* 24:1544–1548.
49. Newell, P. C. 1986. The role of actin polymerization in amoebal chemotaxis. *Bioessays.* 5:208–211.
50. Newman, J., J. E. Estes, L. A. Selden, and L. C. Gershman. 1985. Presence of oligomers at subcritical actin concentrations. *Biochemistry.* 24:1538–1544.
51. Omann, G. M., R. A. Allen, G. M. Bokoch, R. G. Painter, A. E. Traynor, and L. A. Sklar. 1987. Signal transduction and cytoskeletal activation in the neutrophil. *Physiol. Rev.* 67:285–322.
52. Oosawa, F., and M. Kasai. 1962. A theory of linear and helical aggregation of macromolecules. *J. Mol. Biol.* 4:10–21.
53. Pinder, J. C., A. C. Weeds, and W. B. Gratzer. 1986. Study of actin filament ends in the human red cell membrane. *J. Mol. Biol.* 191:461–468.
54. Pollard, T. D., and J. A. Cooper. 1986. Actin and actin-binding proteins. A critical evaluation of mechanisms and functions. *Annu. Rev. Biochem.* 55:987–1035.
55. Scheel, J., K. Ziegelbauer, T. Kupke, B. M. Humbel, A. A. Noegel, G. Gerisch, and M. Schleicher. 1989. Hisactophilin, a histidine-rich actin-binding protein from *Dictyostelium discoideum*. *J. Biol. Chem.* 264: 2832–2839.
56. Schleicher, M., G. Gerisch, and G. Isenberg. 1984. New actin-binding proteins from *Dictyostelium discoideum*. *EMBO (Eur. Mol. Biol. Organ.) J.* 3:2095–2100.
57. Schneider, C., R. A. Newman, D. R. Sutherland, U. Asser, and M. F. Greaves. 1982. A one-step purification of membrane proteins using a high efficiency immunomatrix. *J. Biol. Chem.* 257:10766–10769.
58. Schwartz, M. A., and E. J. Luna. 1986. Binding and assembly of actin filaments by plasma membranes from *Dictyostelium discoideum*. *J. Cell Biol.* 102:2067–2075.
59. Schwartz, M. A., and E. J. Luna. 1988. How actin binds and assembles onto plasma membranes from *Dictyostelium discoideum*. *J. Cell Biol.* 107:201–209.
60. Sherwin, T., and K. Gull. 1989. Visualization of detyrosination along single microtubules reveals novel mechanisms of assembly during cytoskeletal duplication in trypansosomes. *Cell.* 57:211–221.
61. Silverstein, S. C., R. M. Steinman, and Z. A. Cohn. 1977. Endocytosis. *Annu. Rev. Biochem.* 46:669–722.
62. Singer, S. J., and A. Kupfer. 1986. The directed migration of eucaryotic cells. *Annu. Rev. Cell Biol.* 2:337–365.
63. Sklar, L. A., G. M. Omann, and R. G. Painter. 1985. Relationship of actin polymerization and depolymerization to light scattering in human neutrophils: dependence on receptor occupancy and intracellular Ca^{++}. *J. Cell Biol.* 101:1161–1166.
64. Spudich, J. A., and S. Watt. 1971. The regulation of rabbit skeletal muscle contraction. I. Biochemical studies of the interaction of the TM-TN complex with actin and the proteolytic fragments of myosin. *J. Biol. Chem.* 246:4866–4871.
65. Stossel, T. P., C. Chaponnier, R. M. Ezzell, J. H. Hartwig, P. A. Janmey, D. J. Kwiatkowski, S. E. Lind, D. B. Smith, F. S. Southwick, H. L. Yin, and K. S. Zaner. 1985. Nonmuscle actin-binding proteins. *Annu. Rev. Cell Biol.* 1:353–402.
66. Stratford, C. A., and S. Brown. 1985. Isolation of an actin-binding protein from membranes of *Dictyostelium discoideum*. *J. Cell Biol.* 100:727–735.
67. Tellam, R., and C. Frieden. 1982. Cytochalasin D and platelet gelsolin accelerate actin polymer formation. A model for regulation of the extent of actin polymer formation in vivo. *Biochemistry.* 21:3207–3214.
68. Towbin, H., T. Stahelin, and J. Gordon. 1979. Electrophoretic transfer of proteins from polyacrylamide gels to nitrocellulose sheets: procedure and some applications. *Proc. Natl. Acad. Sci. USA.* 76:4350–4354.

69. Tsang, V. C. W., K. Hancock, and A. R. Simons. 1984. Calibration of prestained protein molecular weight standards for use in the western or enzyme linked immunoelectrotransfer blot techniques. *Anal. Biochem.* 143:304–307.
70. Tsukita, S., S. Tsukita, H. Ishikawa, S. Sato, and M. Nakao. 1981. Electron microscopic study of reassociation of spectrin and actin with the human erythrocyte membrane. *J. Cell Biol.* 90:70–77.
71. Wegner, A. 1982. Treadmilling of actin at physiological salt concentrations. An analysis of the critical concentrations of actin filaments. *J. Mol. Biol.* 161:607–615.
72. Wegner, A., and J. Engel. 1975. Kinetics of the cooperative association of actin to actin filaments. *Biophys. Chem.* 3:215–225.
73. Wuestehube, L. J. 1988. Identification and characterization of ponticulin, a 17-kD actin-binding integral glycoprotein from *Dictyostelium discoideum* plasma membranes. Ph.D. thesis. Princeton University, Princeton, NJ. 190 pp.
74. Wuestehube, L. J., and E. J. Luna. 1987. F-actin binds to the cytoplasmic surface of ponticulin, a 17-kD integral glycoprotein from *Dictyostelium discoideum*. *J. Cell Biol.* 105:1741–1751.
75. Wuestehube, L. J., C. P. Chia, and E. J. Luna. 1989. Immunofluorescence localization of ponticulin in motile cells. *Cell Motil. Cytoskeleton.* 13:245–263.
76. Yin, H. L. 1987. Gelsolin: calcium- and polyphosphoinositide-regulated actin-modulating protein. *Bioessays.* 7:176–179.